AGU PUBLICATIONS

JGR

Journal of Geophysical Research: Space Physics

RESEARCH ARTICLE
10.1002/2015JA021008

Key Points:
- Sharp boundary between hot, tenuous and cooler, denser magnetospheric plasma
- Hot plasma consistent with exhaust from near-tail reconnection region
- Sharp boundary drives interchange instability

Correspondence to:
M. F. Thomsen,
mthomsen@psi.edu

Citation:
Thomsen, M. F., D. G. Mitchell, X. Jia, C. M. Jackman, G. Hospodarsky, and A. J. Coates (2015), Plasmapause formation at Saturn, *J. Geophys. Res. Space Physics*, *120*, 2571–2583, doi:10.1002/2015JA021008.

Received 12 JAN 2015
Accepted 6 MAR 2015
Accepted article online 9 MAR 2015
Published online 11 APR 2015

Plasmapause formation at Saturn

M. F. Thomsen[1], D. G. Mitchell[2], X. Jia[3], C. M. Jackman[4], G. Hospodarsky[5], and A. J. Coates[6]

[1]Planetary Science Institute, Tucson, Arizona, USA, [2]Johns Hopkins Applied Physics Laboratory, Laurel, Maryland, USA, [3]Atmospheric, Oceanic, and Space Sciences, University of Michigan, Ann Arbor, Michigan, USA, [4]School of Physics and Astronomy, University of Southampton, Southampton, UK, [5]Department of Physics and Astronomy, University of Iowa, Iowa City, Iowa, USA, [6]Mullard Space Science Laboratory, University College London, Dorking, UK

Abstract Cassini observations during a rapid, high-latitude, dawnside pass from Saturn's lobe to inner magnetosphere on 25 June 2009 provide strong evidence for the formation of a "plasmapause" at Saturn by Vasyliunas-type nightside reconnection of previously mass-loaded flux tubes. A population of hot, tenuous plasma that lies between the lobe and the dense inner magnetospheric plasma is consistent with a region formed by very recent injection from a reconnection region in the tail, including low density, high temperature, supercorotational flow, a significant O^+ content, and the near-simultaneous observation of enhanced Saturn kilometric radiation emissions. The sharp boundary between that region and the cool dense inner magnetospheric plasma thus separates flux tubes that were involved in the reconnection from those that successfully traversed the nightside without mass loss. This event demonstrates that tail reconnection can strip off inner magnetospheric plasma in to at least dipole $L = 8.6$. Clear evidence of flux tube interchange driven by the sharp boundary is found, both inward moving flux tubes of hotter plasma and, for the first time, the outward moving cool population. The outward moving cool regions have azimuthal sizes less than 1 R_S, were probably created within the past 1.2 h, and have outflow speeds greater than about 5 km/s. At the outer edge of the reconnected region, there is also a possible signature of Dungey-type lobe reconnection following the initial Vasyliunas-type reconnection. Observations from this event are entirely consistent with previously described global MHD simulations of tail reconnection, plasmoid departure, and Saturnward injection of reconnected flux.

1. Introduction

The Earth's plasmasphere is a region of cold dense ions of ionospheric origin that encircles the Earth at low L values within the magnetosphere (L is the equatorial crossing point of a dipole magnetic field line through a given point, measured in units of Earth radii, R_E). At the outer edge of the plasmasphere is an abrupt transition, the plasmapause, between the cold dense plasmaspheric plasma and a region of hotter, tenuous plasma known as the plasma sheet and/or ring current. At the plasmapause there can be order-of-magnitude changes in density and temperature on spatial scales of 1 Earth radius or less. The boundary is particularly clear when viewed in electrons with energies approximately a few hundred eV, which largely do not penetrate into the plasmasphere. An explanation for the plasmapause was proposed many years ago [*Nishida*, 1966] as a separatrix in the cold plasma convection pattern created by the superposition of the Earth's corotational electric field (which allows magnetospheric plasma to be dragged in circular orbits around the Earth) and a dawn-to-dusk convection electric field imposed by coupling to the solar wind as it flows past the Earth. In the resulting convection pattern there is a near-Earth region of particle drift paths that close around the planet, allowing ionospheric plasma to accumulate to significant densities; at larger radial distances there is a region of "open" drift trajectories that bring plasma in from the tail, around the inner magnetosphere, and out through the dayside magnetopause, with little time for any ionospheric material to build up. The separatrix between the two is the plasmapause. We now know that this simple steady state picture of the plasmapause as the last closed drift equipotential is rarely realized in practice, but the open-versus-closed drift path paradigm is still the basic underlying physical principle for plasmapause formation at Earth.

At Jupiter and Saturn a similar analysis revealed early on that because of the rapid rotation of those planets and the weak interplanetary electric field, the region of closed drift trajectories (the plasmasphere) should extend all the way to the magnetopause [e.g., *Brice and Ioannidis*, 1970]. The dominant source of magnetospheric plasma at these planets is now known to be moons that orbit in the inner magnetosphere (Io at Jupiter and

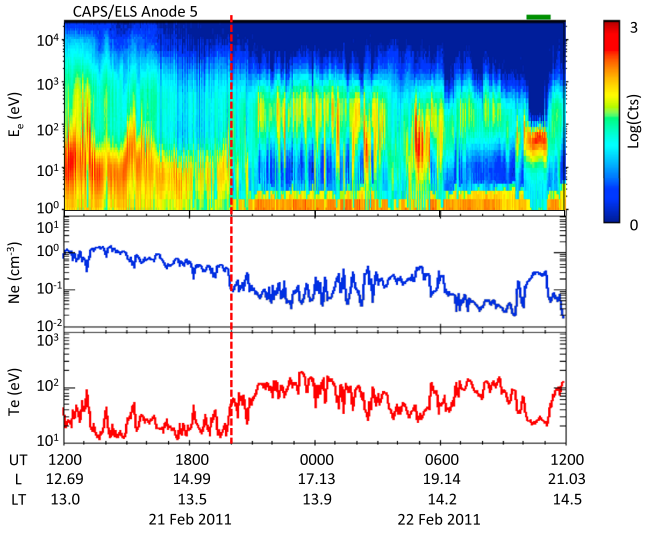

Figure 1. Example of an abrupt transition from cooler, denser inner magnetospheric plasma (prior to ~2000 UT) to hotter, more tenuous plasma (after ~2000). (top) The color-coded electron count rate (proportional to energy flux) from CAPS/ELS as a function of energy and time on 21–22 February 2011. (middle and bottom) The electron density and temperature calculated from the ELS measurements. The red dashed line marks the transition between the two plasma regimes. The interval denoted by the green bar above the spectrogram panel corresponds to a brief entry into the magnetosheath.

Enceladus at Saturn, with an additional contribution of H and H_2 from Titan), producing relatively cool, dense inner magnetospheric material rich in heavy ions (sulfur and oxygen at Io and water group ions at Enceladus). This continuously produced plasma mass must ultimately be shed via outward radial transport to the solar wind [e.g., *Thomsen*, 2013, and references therein]. Thus, one might expect the outer magnetosphere to be filled with relatively cool plasma originating in the inner magnetosphere, transported essentially out to the magnetopause; i.e., we do not expect to see a classical plasmapause like Earth's. Indeed, numerous passes of the Cassini spacecraft through the low-latitude dayside magnetosphere have shown that such cool, dense, water-dominated plasma is frequently observed near the magnetopause.

On the other hand, Cassini also quite commonly encounters clear transitions between cool plasma of inner magnetospheric origin and a hotter, more tenuous population that appears frequently beyond ~10 R_S [e.g., *Schippers et al.*, 2008]. Figure 1 illustrates such a transition, observed on 21–22 February 2011 at a radial distance of 15.7 R_S, a local time of 13.7 LT, and a latitude very near the equatorial plane. The intense electron fluxes at energies below 100 eV early in the interval are characteristic of the cool, dense inner magnetosphere. The dense, warm population near 1100 UT on 22 February, indicated by the green bar above the spectrogram, corresponds to the spacecraft crossing the magnetopause into the magnetosheath. Between these two regions there is a long interval of mostly hot, tenuous electrons, with a few brief intervals of cooler, denser material interspersed. This pass is rather typical, showing a fairly abrupt transition (red dashed line) from the cool inner magnetospheric material to the hotter outer magnetospheric population

The transition from cool, dense to hot, tenuous plasma on this pass is not monotonic; that is, there are numerous brief intervals of cooler, denser material well after the main transition (e.g., ~0230 UT on 22 February), as well as several hotter, more tenuous intervals prior to the main transition. This variability is attributable to two factors: (1) the operation of the centrifugally driven interchange instability, which is known to be one of the primary transport processes removing moon-produced charged particles from the inner to the outer magnetosphere, and (2) the fact that corotational flow is continually moving new longitude sectors across the spacecraft trajectory, each reflecting its own stability history. In addition, there is a background population of hot electrons throughout the entire interval, in both the cool and warm regions, presumably spread throughout all longitude sectors by gradient and curvature drift relative to the corotation.

Based on plasma observations during Cassini's orbital insertion, *Young et al.* [2005] referred to the cold, dense region in Saturn's inner magnetosphere as the "inner plasmasphere" and the transition from that to the lower density, hotter population seen characteristically in the outer magnetosphere as "a plasmapause that represents the last closed equipotential of plasma flow around the planet." In contrast to the situation at the Earth described above, Young et al. attributed the last closed equipotential not to the superposition of the corotation and convection electric fields but to the disruption of plasma-laden flux tube drifts by a centrifugally driven process in which the flux tubes break open and spill their contents down the tail. In this picture, the hot, tenuous plasma of the outer magnetosphere is what is left over from this disruption process [see also *McAndrews et al.,* 2009]. At Jupiter, this region has been termed the "cushion region"

[*Kivelson and Southwood*, 2005]. It is characterized there by a change from a stretched magnetodisk field orientation back toward a more dipolar one, but a search for such a magnetic signature at Saturn has been unsuccessful [*Went et al.*, 2011].

Vasyliunas [1983] hypothesized such a rotationally driven mass loss process at Jupiter as a quasi-steady pattern of magnetic reconnection, with a neutral line extending across a segment of the magnetospheric tail. Plasma in the disconnected portion of a flux tube would flow away downtail on the tailward side of the neutral line, while the plasma that remained on the shortened flux tube would flow sunward and around the dawnside of the inner magnetosphere. Subsequent observations within the magnetospheric tail [e.g., *McAndrews et al.*, 2009; *Jackman and Arridge*, 2011; *Thomsen et al.*, 2013, 2014a; *Kane et al.*, 2014] show no evidence of a quasi-steady neutral line within or near the region explored by Cassini, but there is a great deal of evidence for the occurrence of transient tail reconnection events, which release a plasmoid downtail and produce dipolarization and plasma heating as the depleted flux tube snaps back toward the planet [e.g., *Jackman et al.*, 2014, and references therein]. Global MHD simulations also show clear evidence for the occurrence of tail reconnection, plasmoid production, and injection of heated remnant plasma into the near planet region [*Zieger et al.*, 2010; *Jia et al.*, 2012].

Thus, it is plausible to follow *Young et al.* [2005] and identify the transition from cool inner magnetospheric plasma to warm outer magnetospheric plasma as a "plasmapause" that separates drift trajectories that successfully close around the planet without experiencing tail reconnection from those that do encounter the reconnection region. Note that this boundary is distinctly different from the density transition previously referred to as the "plasmapause-like density boundary" by *Gurnett et al.* [2010], which was found to be associated with the open/closed field line boundary. In the case shown in Figure 1, both the cooler population and the hotter population are clearly on closed magnetic field lines (evidenced by the substantial fluxes of particles and the mirror symmetry of the distribution with respect to the magnetic field, not shown), as are the populations found on either side of the terrestrial plasmapause.

One other interesting aspect of what we are here terming the plasmapause is that the hotter, more tenuous plasma returned from the reconnection region should coat the region of closed drift trajectories, forming a strong inward gradient of the flux tube content, which is unstable to centrifugally driven interchange motion. The result should be fingers of cool dense plasma moving out into the hot tenuous region and vice versa. This boundary is thus a likely point of origin of the interchange injections seen commonly in Saturn's inner magnetosphere ($<\sim 10\,R_S$), as suggested by *Mitchell et al.* [2015].

In this paper we present Cassini observations from a high-latitude inbound pass, which, because of the convergence of the magnetic field lines, allows a rapid scan through the entire closed field portion of the magnetosphere from the inner edge of the lobe (i.e., the region of open field lines with one end in Saturn's polar cap ionosphere and the other in the solar wind, characterized by extremely low particle fluxes) to the inner, cool dense plasma region. During this crossing we find that between the lobe and the inner region of dense cool plasma, there is a region of hot, tenuous plasma, with a sharp boundary separating it from the cooler region. The hot plasma is consistent with very recent injection from a reconnection region in the tail, and we interpret the sharp boundary between that and the cool dense plasma as the plasmapause described above, separating flux tubes that were involved in the reconnection from those that successfully traversed the nightside without mass loss. Thus, this dawnside crossing provides direct evidence for the formation of the plasmapause boundary at Saturn and indicates the depth to which tail reconnection can strip off inner magnetospheric plasma, at least for this one measurement. We also see evidence of the subsequent occurrence of the interchange instability at this newly created plasmapause.

2. Observations

Data for this study come from several instruments on Cassini: the Cassini Plasma Spectrometer (CAPS) [*Young et al.*, 2004], the Cassini Magnetic Field Investigation (MAG) [*Dougherty et al.*, 2004], the Magnetosphere Imaging Instrument (MIMI) [*Krimigis et al.*, 2004], and the Cassini Radio and Plasma Wave Investigation (RPWS) [*Gurnett et al.*, 2004].

On 25 June 2009 Cassini was inbound toward Saturn near 9 LT at relatively high southern latitudes ($-30°$ to $-20°$ during the interval of interest here). Figure 2 shows the orbit projected onto the *X-Y*, *X-Z*,

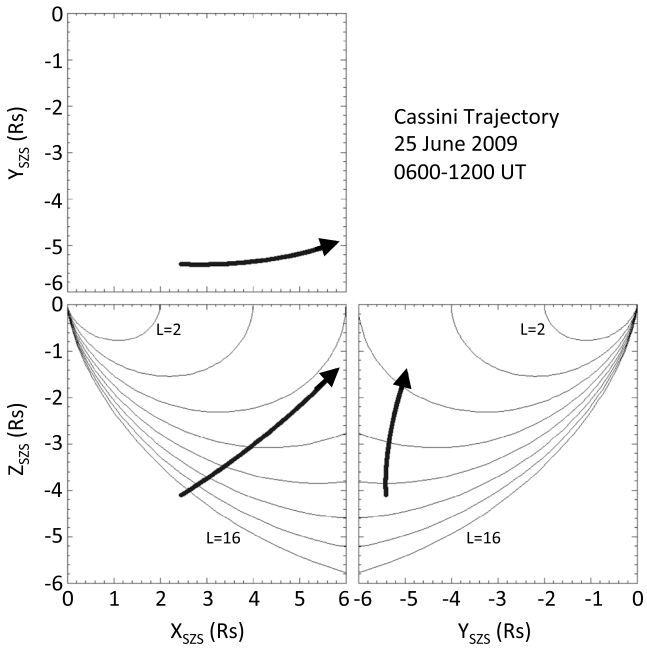

Figure 2. Cassini trajectory (heavy arrow) for 0600–1200 UT on 25 June 2009, projected onto the *X-Y*, *X-Z*, and *Y-Z* planes of the Saturn Equatorial coordinate system (SZS). Dipole field lines at $L = 2$ and $L = 16$ are labeled.

and *Y-Z* planes of the Saturn equatorial coordinate system (SZS). Also shown for reference are dipole magnetic field lines at intervals of 2 in *L*.

Figure 3 presents an overview of the observations during 6 h of this pass. From Figures 3a to 3h, the figure shows the ion and electron energy flux spectrograms from the CAPS Ion Mass Spectrometer (IMS) and Electron Spectrometer (ELS), the values of the radial, theta, and phi components of the magnetic field from MAG, the proton and O^+ flux spectrograms from MIMI/Charge-Energy-Mass Spectrometer, and the electric field power spectrum from RPWS. At the high latitude of the trajectory on this pass, magnetic L shells are close together, and as will be detailed below, Cassini passed from the lobe to the inner magnetosphere within just a few hours.

At the beginning of the interval in Figure 3, the spacecraft was on open magnetic field lines in the magnetospheric lobe, as indicated by the extremely low electron fluxes seen in CAPS/ELS above ~20 eV in Figure 3b. The high fluxes seen at lower energies in Figure 3b are spacecraft photoelectrons trapped in the spacecraft potential well. The lobe identification is confirmed by the strong and relatively smooth magnetic field (Figures 3c–3e) and by the very low fluxes of energetic ions seen in Figures 3f and 3g.

At ~0728 UT (indicated by the magenta dashed line labeled "1"), electron fluxes in the energy range of a few hundred eV to 2 keV appeared, coincident with the beginning of a field rotation seen most clearly in the phi component (Figure 3e), as well as the abrupt onset of enhanced energetic H^+ fluxes (Figure 3f). CAPS viewing at this time extended from pitch angles of ~45° to 180°, and the electron fluxes were symmetric about 90°, indicating closed field lines. At ~0738 UT (magenta line "2"), the electron fluxes increased further and extended to higher energies. At about the same time there was an onset of energetic O^+ ions (Figure 3g), and very faint fluxes of ions at lower energy became visible (Figure 3a). The energetic H^+ fluxes also increased there.

Thereafter, Cassini saw a progressively denser and hotter electron population and increasing fluxes of energetic ions until ~0910 UT (magenta line "3"), at which time there was an abrupt change in the character of the plasma ions and electrons, from the hot and tenuous population to a cooler, denser population characteristic of the inner magnetosphere. The temporal modulation of the ion fluxes after time 3 in Figure 3a is produced by the motion of the CAPS actuator swinging the field of view alternately into and out of the plasma flow direction. Further, in the cooler region after 0910 UT, there are two distinct peaks in the energy distribution, corresponding to populations of light ions (H^+ and H_2^+) and W^+ (water group ions: O^+, OH^+, H_2O^+, and H_3O^+) flowing at a common convection speed.

Figure 4 shows the computed electron density and temperature [e.g., *Lewis et al.*, 2008], density and temperature of the three dominant plasma ion species [e.g., *Thomsen et al.*, 2010], and fluxes of energetic H^+ and O^+ ions in two different energy ranges for the same time interval. The CAPS viewing at this time was not ideal, with the corotation direction barely at the edge of the field of view, so the ion densities are probably underestimated by the numerical integration algorithm used for the moments. The apparent decline in ion densities after ~1030 UT is due to a worsening of the viewing associated with a spacecraft rotation at that time. Nonetheless, the traces in Figure 4 confirm the general conclusions from Figure 3 that the particle populations exhibited discrete changes at the three times marked by magenta dashed lines, which are the same as those in Figure 3.

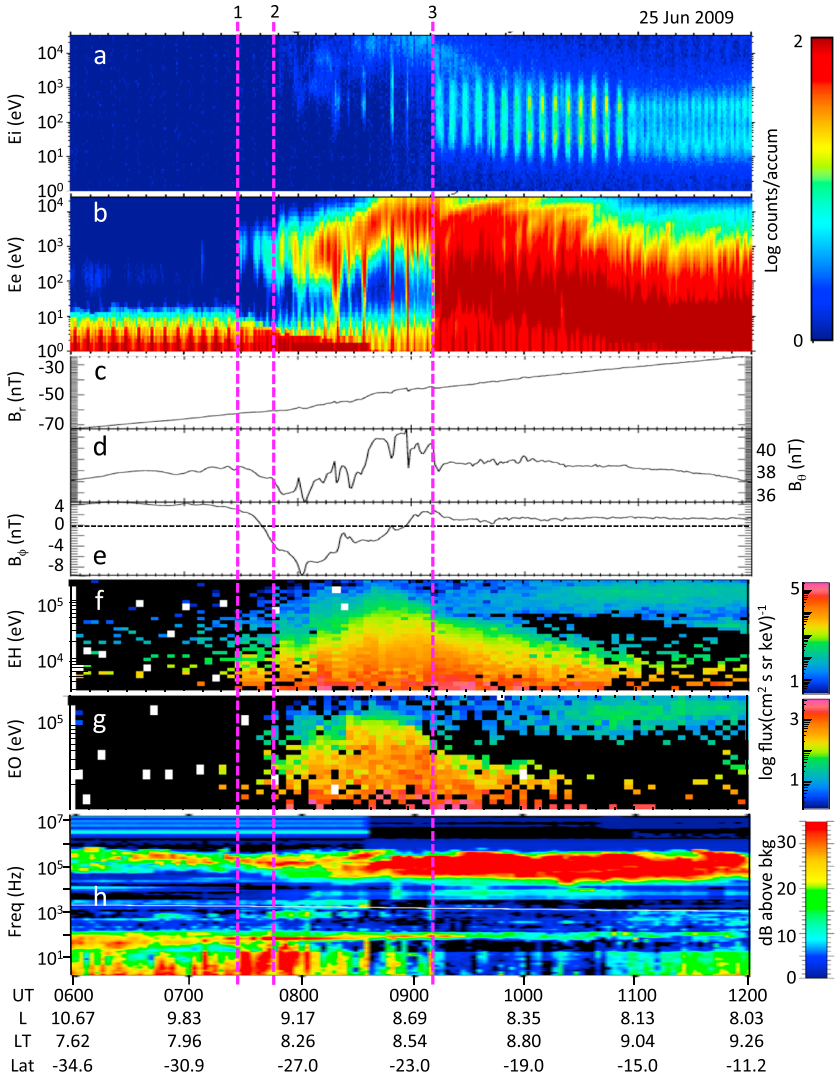

Figure 3. Overview of Cassini observations on 25 June 2009: (a and b) color-coded count rates (proportional to energy flux) of ions and electrons, respectively, from CAPS/IMS/SNG and CAPS/ELS, averaged over all eight anodes; (c–e) r, θ, and ϕ components of the magnetic field measured by MAG; (f and g) flux of energetic H^+ and O^+ ions, respectively, from MIMI; and (h) electric field power spectrum measured by RPWS. Time 1 marks Cassini's exit from the open field lines of the lobe into the region of closed field lines. Time 3 marks the abrupt transition from hot, tenuous plasma into cool, dense, inner magnetospheric plasma. The interval between Time 1 and Time 2 may correspond to outflow from lobe reconnection (see section 3).

Figure 4c quantifies the clear presence of energetic O^+ ions between time 2 and time 3 noted in Figure 3. Moreover, in the ion moments (Figures 4a and 4b) there is some evidence for the presence of water group ions in this region, although the low fluxes prevent reliable determination of the W^+ properties. The presence of W^+ is confirmed by time-of-flight measurements from CAPS, as shown in Figure 5, which shows the contributions to the density in each CAPS/time-of-flight (TOF) energy channel determined under the assumption of isotropy as described by *Thomsen et al.* [2014b]. Figure 5a shows TOF measurements before the sharp transition at t3, and Figure 5b shows the same analysis for the interval immediately after the t3 transition. The numbers in parentheses show the densities of each species calculated by summing the contributions from all the energy channels. Because of the unsatisfactory viewing mentioned above, as well as the clear anisotropy of the observed ions, these estimates are not quantitatively accurate, but they serve to highlight the significant jump in densities across the t3 transition, as well as the appreciable presence of W^+ in the hot region prior to the transition. The spectral shape of the hot plasma outside the t3 boundary

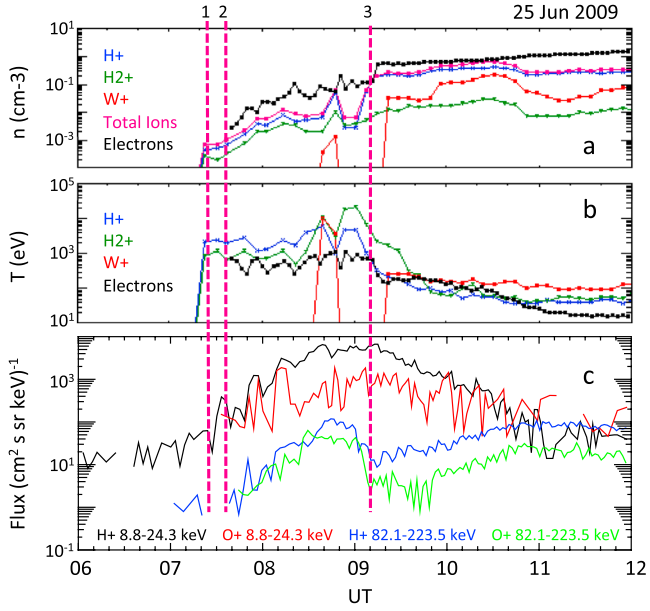

Figure 4. (a) Numerically integrated densities and (b) temperatures of ions and electrons observed by CAPS on 25 June 2009; (c) observed fluxes of energetic ions (black: H^+ 8.8–24.3 keV; red: O^+ 8.8–24.3 keV; blue: H^+ 82.1–223.5 keV; green: O^+ 82.1–223.5 keV). The times marked are the same as those in Figure 3.

(Figure 5a) is similar to that of the suprathermal (above ~3 keV) population seen in the ion distribution inside the boundary (Figure 5b), possibly suggesting a common origin.

The ion distributions seen after the t3 boundary crossing are quite characteristic of the inner magnetospheric population in density, temperature, and composition (the H^+ density dominates over W^+ at high latitudes due to the strong equatorial confinement of the heavier ions [e.g., *Thomsen et al.*, 2010]). Bulk flow moments computed separately for the H^+ and W^+ populations (not shown here) give a dominantly azimuthal flow velocity in this region at speeds ~80% of corotation, consistent with typical values seen inside of $L \sim 10$ [e.g., *Wilson et al.*, 2008, 2009].

Returning to Figure 3, within the hot plasma region between ~0728 and ~0910 UT (between t1 and t3), there were at least four very brief intervals of cooler, denser material with properties similar to those in the inner magnetosphere after 0910 UT (~0820, ~0835, ~0850, and ~0858 UT). In addition, though more difficult to see, there are a few very brief intervals after 0910 where the electron temperature is significantly higher than the adjacent ambient plasma (e.g., 1040 UT). These brief intervals, both before and after time 3, have properties quite similar to those of the plasma on the opposite side of the t3 boundary, strongly suggesting that they are the result of interchange motions spawned by the sharp gradient in flux tube content at that boundary. The cool plasma intervals within the hot region outside of the t3 boundary thus may represent the first reported observations of the outward propagating fingers of dense plasma associated with the interchange instability; previous analyses of interchange have focused entirely on the

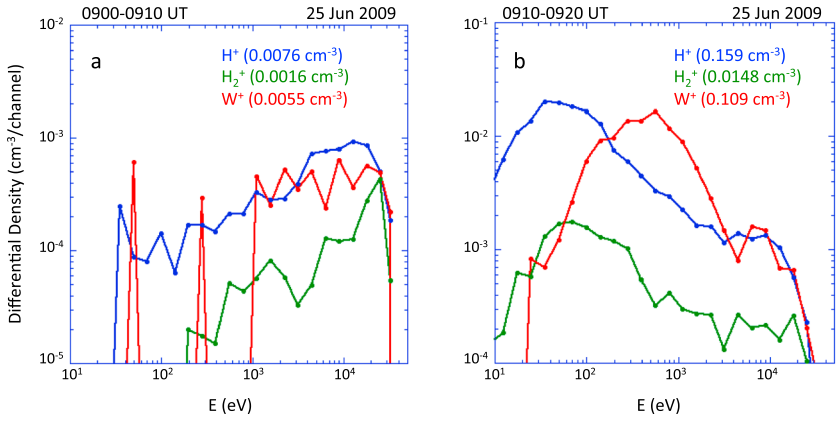

Figure 5. Differential contributions to the density of each species (H^+, H_2^+, and W^+) within each CAPS/IMS/TOF energy channel for two intervals on 25 June 2009. The differential densities are derived from time-of-flight measurements as described by *Thomsen et al.* [2014b]. Color-coded numbers in the legend of each panel give the integrated densities derived by summing the differential contributions. (a) The first interval is prior to the transition at time 3 in Figures 3 and 4, and (b) the second interval is after that transition. Despite the obvious spectral differences between the two intervals, they both contain a substantial fraction of water group ions.

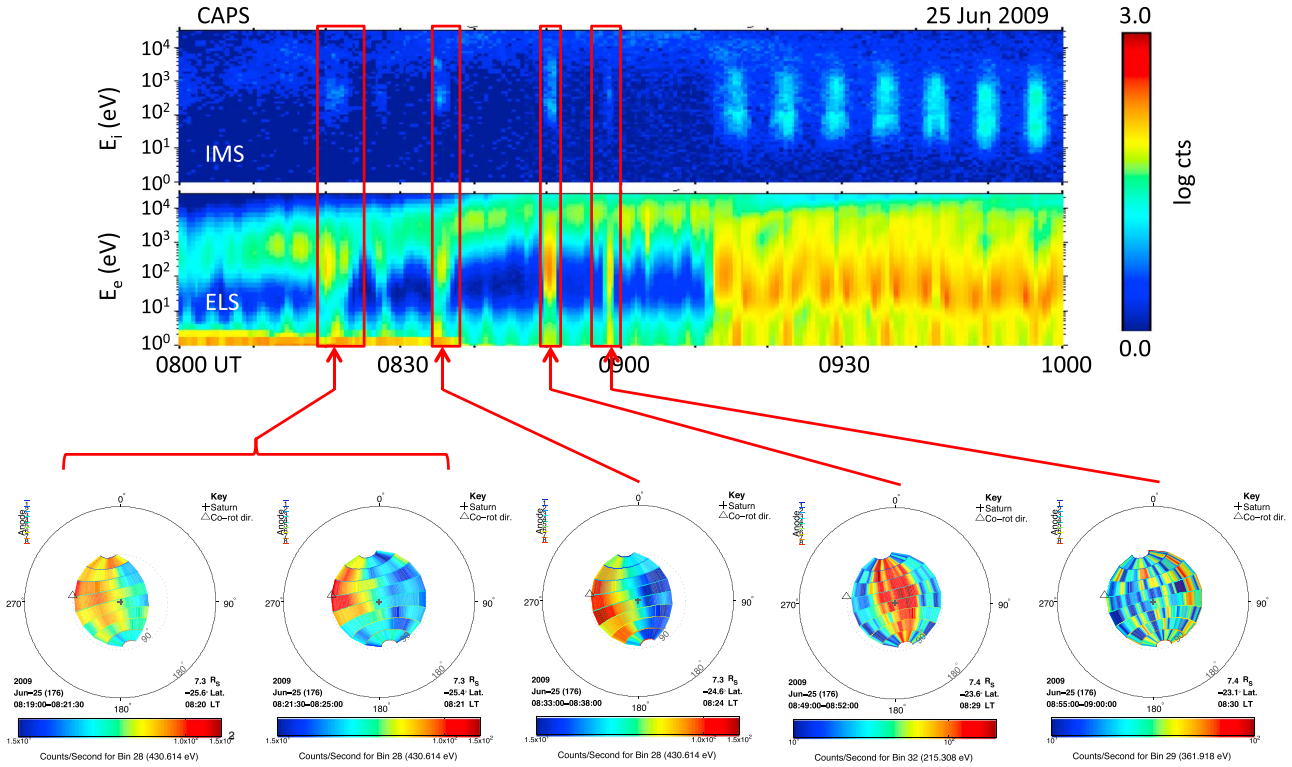

Figure 6. Expanded view of the brief intervals of cool, dense plasma observed within the hot, tenuous region prior to the transition at t3 in Figure 3 (~0912 UT). (top) The ion and electron count rates from CAPS as a function of energy and time, and (bottom) the five panels show all-sky angular distributions of ions at the four indicated intervals, taken at the energy of peak ion counts. The center of the angular distributions corresponds to the look direction toward Saturn, and the open triangle halfway to the outer circle on the left of center corresponds to the look direction into corotation. The first three angular distributions show counts peaking near the corotation direction, the fourth panel peaks near the Saturn direction (outflow), and the fifth panel shows no clear anisotropy.

fingers of hot plasma that penetrate into the inner magnetosphere. We use the term "fingers" for these structures in spite of the fact that a single-point measurement does not allow unambiguous distinction between extended fingers and isolated flux tubes or "blobs" of plasma. A similar ambiguity existed for many years in studies of so-called "detached plasma regions" at the Earth, which were ultimately shown via global imaging to be distended tails or plumes of plasmaspheric material that were still attached to the larger plasmaspheric body [e.g., *Sandel et al.*, 2001]. Moreover, numerical simulations of the interchange instability in the inner magnetosphere of Saturn [e.g., *Liu et al.*, 2010] reveal both inward and outward flowing fingers of interchange plasma, with little evidence for disconnection from the main plasma reservoirs on either side of the unstable boundary. However, we should bear in mind that from the Cassini observations alone, the structure of these cool plasma intervals cannot actually be discerned.

Although not shown in Figure 3, we also find that the magnetic field magnitude within some of these cold plasma fingers is depressed relative to the ambient field, indicating that the pressure in the cold, dense plasma exceeds the ambient hot plasma pressure. Magnetic signatures of pressure imbalance have previously been described for inner magnetosphere interchange events [e.g., *André et al.*, 2007].

Figure 6 shows an expanded view of the cool intervals outside the t3 boundary. In Figure 6 (bottom) the five panels show all-sky views of cuts through the observed ion distributions at the energy corresponding to the peak counts in each interval. The center of each circle corresponds to the look direction toward Saturn, and the open triangle to the left of center corresponds to the look direction into corotation. These intervals are too brief to cleanly resolve the distribution with the CAPS actuation (i.e., it is difficult to distinguish a flow anisotropy from simple time aliasing of a short-lived burst), but for the events at ~0820 and ~0835 UT, the flow appears to be coming from the corotational direction, while that at ~0850 peaks in the outward flowing direction. The event at ~0900 has no discernible anisotropy and may be one that was so brief that IMS just caught an edge of the population. The lack of a clear outward flow component during the events at 0820

and 0835 suggests that the instability-driven outflow either has concluded by the time of the observation of these features or has slowed to the point that it is no longer the dominant velocity component in the general corotational flow of the ambient medium. For the outflowing event at 0850, Cassini may be measuring it while the outflowing component is still the dominant component of the flow.

Assuming that the older cool dense intervals observed within the hot plasma are flowing at the same velocity as the ambient material, they offer an opportunity to determine the flow speed of the hotter plasma, which otherwise is too weak, too hot, and too isotropic for a credible velocity determination. For example, if we approximate the observed ion energy distribution at 08:35:29 as the superposition of H^+ and W^+ Maxwellian distributions moving with the same flow speed, we find a reasonable match to the location and width of the two observed IMS peaks with a flow speed ~160 km/s and temperatures for H^+ and W^+ ~59 eV and 305 eV, respectively. While there is considerable uncertainty in these values, examination of the count rate spectrum makes it quite clear that the flow speed must be substantially greater than the local corotation speed at Cassini's location (~64 km/s). The inferred W^+ temperature is essentially the same as estimated by the numerical moments calculation at ~09:30, shortly after Cassini entered the cooler plasma region. The inferred H^+ temperature is about a factor of 2 lower than the later numerical moments, but the latter may be elevated because of the presence of suprathermal H^+ evident in Figure 3. In any case, this analysis shows that the brief cool plasma intervals are consistent with inner magnetospheric plasma flowing azimuthally at a speed well above corotation. We infer that the surrounding hot plasma is similarly supercorotating in this region. Such supercorotation is an expected signature of outflow from a reconnection region [e.g., *Masters et al.*, 2011].

The observed magnetic field components (Figures 3c–3e) support the conclusion that plasma within the hotter region before t3 was flowing faster than corotation: In particular, the extended interval of $B_\varphi < 0$ (07:40–08:55) while B_r was also negative shows that the field was "leading," i.e., bent forward out of the dipole meridian plane throughout almost all of the interval, a signature that previously has been attributed to supercorotational flow [e.g., *Khurana and Kivelson*, 1993; *Bunce et al.*, 2003].

Finally, Figure 3h shows that at approximately the same time as Cassini entered the closed field line region (t1), RPWS saw an expansion to lower frequencies and a subsequent intensification of the band of waves associated with Saturn kilometric radiation (SKR) (above ~10^4 Hz). Such wave signatures have been previously associated with tail reconnection, injections of energized ions from the tail, and auroral intensification [e.g., *Mitchell et al.*, 2005, 2009; *Jackman et al.*, 2009]. Because of possible viewing limitations associated with the beaming of SKR [e.g., *Lamy et al.*, 2008], the SKR intensification may actually have started somewhat earlier than the time at which it was observed, with some delay until the emission cone rotated to where Cassini could begin to see it. Thus, we cannot use the observed onset as a fiducial marker for when the reconnection may have begun, but its occurrence in association with the other observations serves to confirm that tail reconnection and dipolarization of reconnected flux are involved in producing the observed hot plasma region.

3. Discussion

In keeping with the picture developed in section 1, we interpret the sequence of observations described above as follows. The region of cool, subcorotating inner magnetospheric plasma encountered after t3 is the outermost extent of mass-loaded flux tubes that have successfully traversed the nightside region without disruption. Beyond the t3 boundary, the more tenuous, hotter, supercorotating plasma corresponds to flux tubes that have experienced reconnection and loss of mass as they passed through the nightside. The presence of substantial amounts of water group ions on those flux tubes demonstrates that the reconnection was of the Vasyliunas type, i.e., the reconnected flux tubes were originally closed and filled with inner magnetospheric plasma but were stretched to the point of pinching off during their nightside passage. Thus, the t3 boundary corresponds to Saturn's plasmapause, separating the last closed flow path around the planet from flow paths that have encountered the disruption of tail reconnection, as originally described by *Young et al.* [2005]. The dipole L shell at which this boundary occurs ($L = 8.6$) thus gives an indication of how deeply the tail reconnection can at times penetrate to strip away inner magnetospheric plasma. Of course, the equatorial mapping of this boundary would lie beyond 8.6 R_S due to the distention of the magnetic field by the ring current and tail current, especially on the nightside, consistent with energetic neutral atom observations, which suggest that tail reconnection probably occurs at or beyond 15 R_S. However, the dipole L

value of the boundary observed by Cassini at relatively high latitude is probably a good indicator of where ionospheric signatures of the phenomenon should be found.

Our identification of the hot plasma interval between t1 and t3 as the outflow from a tail reconnection region is strengthened by the clear similarity of the plasma properties to those in previously reported dipolarization events [*Bunce et al.*, 2005; *Thomsen et al.*, 2013]. The magnetic signature (increase in B_θ; transition from "bent-back" to "bent-forward" orientation) is also quite similar to that exhibited by the Bunce et al. injection event and to dipolarizations reported by *Russell et al.* [2008] and *Jackman et al.* [2013]. The importance of the present event is that it clearly shows the evolution of the injected plasma, i.e., that it coats the inner undisturbed plasma region well into the dayside magnetosphere, forming the so-called cushion region.

The sharp gradient in the flux tube content associated with the plasmapause boundary is very likely unstable to the growth of centrifugally driven flux tube interchange, and this crossing provides direct evidence consistent with such an instability: We see clear evidence of inclusions of hot, tenuous plasma in the inner, cooler region and of cool, dense, inner magnetospheric plasma within the hotter, tenuous outer region. While it is possible that there may be some other explanation for the presence of these brief "alien" plasma intervals on either side of the main transition (e.g., patchiness of the nightside reconnection process), they seem entirely consistent with the expectations of interchange occurring at the boundary between the cool and hot plasma. Within this scenario, the cool plasma regions seen outside the boundary represent the first reported outward moving interchange fingers at Saturn. At the inferred azimuthal flow speed of 160 km/s for the cool plasma at 08:35:29, the 2 min duration of the event yields a transverse width ~0.3 R_S. Further, if we assume that the reconnection event that created the unstable density gradient occurred near 02 LT, we find a lifetime for the interchange fingers of something less than 1.2 h since at least two of the events no longer have a discernible outward flow component. Travel from the plasmapause at $L = 8.6$ to the outermost point at which cool plasma is clearly seen, $L = 9.0$ at 0820 UT, would then require a flow speed of at least 5 km/s.

The inferred width of the outflow fingers is comparable to that of the inward moving interchange events studied by *Chen and Hill* [2008]. Based on their simulations of the interchange instability, *Liu et al.* [2010] argued that the outflow channels are broader and slower than the inflow channels, in contrast to this finding. However, they were primarily describing the late time (~steady state) conditions in their simulations, whereas the interchange events we are observing here are quite young and should be compared with the early time outflow channels in the Liu et al. simulations, which do appear to be similar in azimuthal extent to the inflow channels.

The scenario described above is further supported by global MHD simulations. Figure 7 shows *X-Y* and *Y-Z* projections of plasma and field properties extracted from the MHD simulation reported in section 3.2.2 of *Jia et al.* [2012], in which they found clear evidence for episodes of tail reconnection, plasmoid production, and dipolarization of reconnected flux tubes. The simulations described by *Jia et al.* [2012] were not intended to reproduce any specific observed event but rather to illustrate the physics of the magnetospheric evolution under conditions of centrifugal stress from inner magnetospheric mass loading. To compare with the Cassini observations described above, the panels in Figure 7 are taken from time step $T = 372$ h during the simulation, approximately 2 h after the onset of tail reconnection near 02 LT at $L = 25\ R_S$. To produce Figure 7, the Cassini trajectory from 25 June 2009 described above was traced through the $T = 372$ h snapshot of the simulation.

Figure 7a shows color-coded contours of the plasma temperature in the *X-Y* plane. The red region that extends from ~02 LT around the dawnside of the magnetosphere to ~09 LT is very hot plasma that was injected sunward from the tail reconnection region. The green and red radial lines in the postdawn sector are projections of the magnetic field through Cassini's trajectory at three different points during its passage through the region in which the observations described above were obtained. These field line projections are color coded according to the value of $V_\varphi/V_{\mathrm{corot}}$ at their equatorial foot point. The red field line, indicative of strong supercorotation, maps to the hot, injected plasma, while the green field line just interior to it maps to the cooler, nearly corotating plasma inward of the injection.

In Figure 7b, the *Y-Z* projection of the trajectory is plotted, with the same field lines colored according to $V_\varphi/V_{\mathrm{corot}}$. In addition to the near-corotational green field lines at lower L and the supercorotating red lines at slightly higher L, the blue traced line is an open lobe field line. The trajectory itself is color coded according to the local value of B_φ. Thus, if one follows the spacecraft trajectory inbound (counterclockwise) from

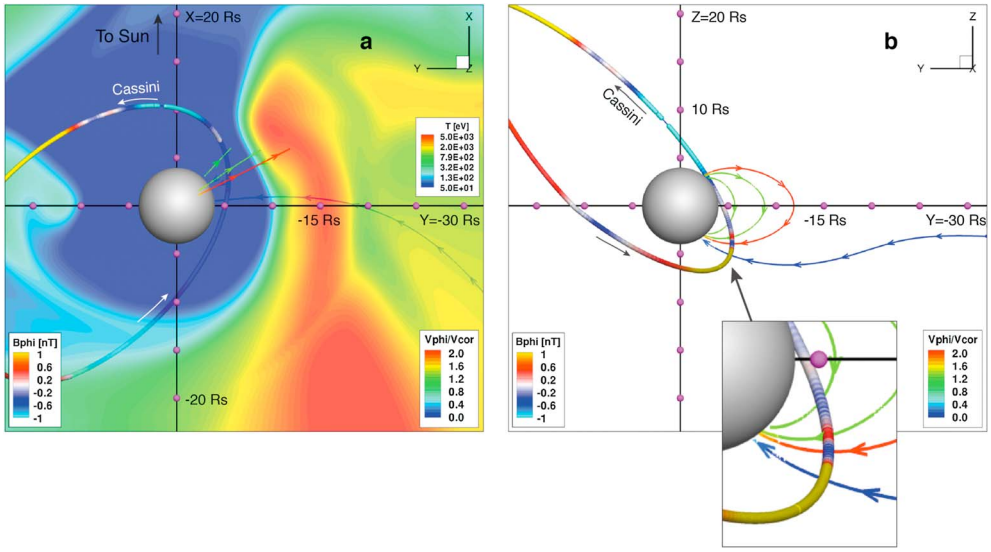

Figure 7. Output from a global MHD simulation of Saturn's magnetospheric dynamics by *Jia et al.* [2012]. (a) Color-coded plasma temperature in the *X-Y* plane at time $T = 372$ h in the simulation, with the Cassini trajectory on 25 June 2009 projected into the plane and color coded according to the local simulation value of B_φ along the trajectory. Four field lines through the trajectory are similarly projected into the plane and color coded according to the azimuthal flow velocity at their equatorial crossing, measured relative to the corotation speed there. The plasma in the red (hot) channel on the dawnside of the magnetosphere is supercorotating (red field line), while the cooler plasma at lower *L* is more nearly corotating (green field lines). The blue traced field line is only connected to the southern ionosphere and lies entirely below the equatorial plane. (b) Cassini trajectory and traced field lines projected onto the *Y-Z* plane, with the same color coding for the field lines as in Figure 7a (based on the flow speed) and of the trajectory (based on the local value of the azimuthal component of the magnetic field). As the trajectory crosses the red (i.e., fast flowing) field line, B_φ goes negative (blue), as also seen in the Cassini observations on 25 June 2009.

$(y, z) \sim (-4, -7)$, one first encounters lobe field lines with essentially no azimuthal flow velocity (color coded blue) and positive B_φ (trajectory color coded gold), indicating a swept-back orientation (see expanded view in inset of Figure 7b). The spacecraft then passes into the closed field region, initially into plasma that is strongly supercorotating and with a negative value of B_φ (the brief blue portion of the trajectory through the red field line), indicating a swept-forward field geometry. It then passes into the nearly corotating green line region, where B_φ is briefly positive (red trajectory segment), then relaxes toward zero.

In essentially all respects the simulation shown in Figure 7 produces field and plasma signatures in accord with those observed by Cassini on 25 June 2009. It also offers further insight into the dynamics of the tail reconnection process. As discussed by *Jia et al.* [2012], the reconnection in the simulation not only produced a plasmoid and corresponding Saturnward injection, but it also grew to involve lobe field lines as well, thereby passing from Vasyliunas-type reconnection to Dungey type, in which open flux is closed and returned to circulate through the dayside magnetosphere. It is this passage from reconnection on closed to open field lines that allows the strong tailward ejection of the plasmoid [e.g., *Jia et al.*, 2012; *Thomsen et al.*, 2013; *Mitchell et al.*, 2015], in addition to providing for episodic closure of polar cap flux. In the *Jia et al.* [2012] simulation, reconnected previously open flux forms a layer outside of the region of reconnected but previously closed flux emerging from the tail reconnection region.

Figure 8 explores the evidence for lobe closure (i.e., Dungey-type reconnection) in the simulation of *Jia et al.* [2012]. Figure 8a shows the same plasma temperature plot as Figure 7a, with the same three closed field lines traced from the Cassini trajectory down to the ionosphere. In addition, the equatorial foot points of these closed field lines have been traced backward in the flow field of this snapshot of the simulation ($T = 372$ h). If the flow patterns were approximately constant over the previous 2 h, the grey arrowed lines would show the trajectories followed by the flux tubes encountered at the three locations P1–P3. The trajectory from point P1, well within the hot sunward flowing population, traces back to a point where the field line is no longer closed, i.e., to a site of Dungey-type reconnection. By contrast, back trajectories from both P2 and P3 remain on closed field lines through the tail region. The trace from P3 remains always within the cool,

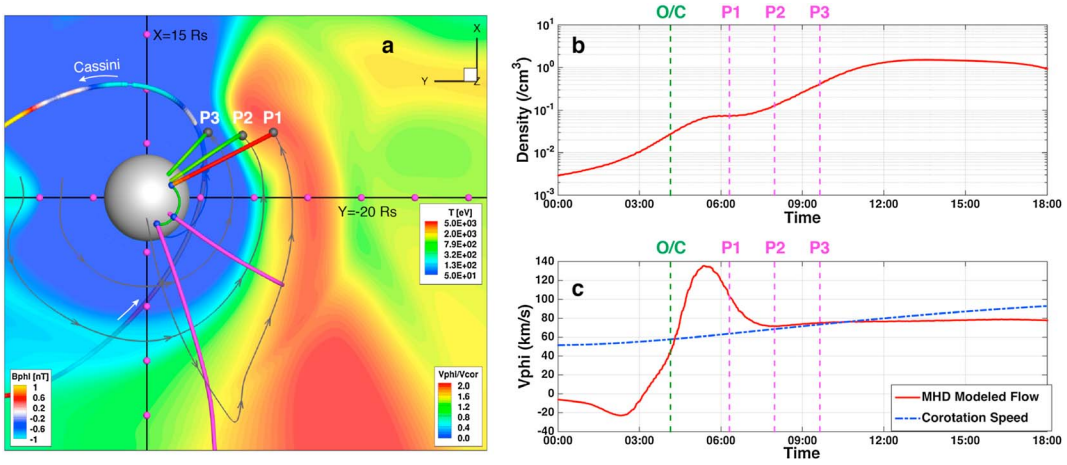

Figure 8. Plasma parameters along the Cassini trajectory flown through a snapshot of the global MHD simulation of *Jia et al.* [2012]: (a) Same color-coded temperature plot as shown in Figure 7a, (b) modeled plasma density along the Cassini trajectory, and (c) azimuthal component of the modeled flow velocity along the Cassini trajectory (blue dashed line shows the local full corotation speed). Grey arrowed lines in Figure 8a show the back-traced trajectories of the equatorial foot points of three locations (P1–P3) along the Cassini trajectory, assuming the flow field of the snapshot was approximately constant over the preceding 2 h. The green curve at low altitude is the ionospheric projection of the tracing from point P1, and the two pink lines are the field lines traced outward from that ionospheric foot point every hour. The back-traced trajectory of P1 ultimately traces back to a point where the field line was open, whereas the field lines of P2 and P3 were closed throughout the tracing interval. The Cassini encounter times with P1–P3 are indicated by the dashed magenta lines in Figures 8b and 8c. The green dashed line in Figures 8b and 8c shows the open/closed field line boundary in the simulation in this snapshot.

presumably undisturbed inner magnetosphere plasma. The trace from P2, which is at the edge of the strongly heated region and thus apparently has been energized in the reconnection, also does not make the transition to open field lines. Hence, we identify it as plausibly a product of the Vasyliunas-type internal reconnection of previously closed field lines.

Figures 8b and 8c show plasma parameters along the Cassini trajectory through this snapshot of the simulation. Figure 8a shows the plasma density, and Figure 8b shows the plasma flow speed. The green dashed vertical lines indicate where the Cassini trajectory crosses the open/closed field line boundary in the simulation. The locations of the three traced points are indicated by magenta dashed vertical lines. Figures 8b and 8c show that P1, on reconnected lobe field lines as discussed above, has a higher density than in the lobe proper (left of the o/c boundary), as well as a flow speed much faster than corotation (given by the blue curve in Figure 8c). Point P3, from the unperturbed inner region, exhibits a relatively high density and a flow speed close to corotation. Point P2 shows values intermediate between the reconnected lobe (high *V*phi, low density) and the unperturbed closed region (low *V*phi, high density), consistent with depleted flux tubes returning from the nightside Vasyliunas reconnection of previously filled magnetospheric flux.

As illustrated in Figure 8, the Dungey-cycle layer (P1) is characterized by a lower density than in the Vasyliunas-cycle region inward of it (P2). It should also be largely absent of water group particles, although the simulation does not treat different species. By reference to Figure 4, we therefore speculate that the brief interval between t1 and t2 in the 25 June 2009 event, in which the field lines were probably closed but the densities were quite low and there was very little O^+, may have been such a region of newly closed lobe flux, although the low densities and lack of O^+ might also simply be a consequence of the general decline of fluxes with increased latitude and radial distance. Previous evidence for lobe reconnection has been seen in the occurrence of the postplasmoid plasma sheet [e.g., *Jackman et al.*, 2011], interpreted as the northward pointing field lines with both ends in the solar wind that drape a departing plasmoid (see also the discussion in *Jia et al.* [2012]). The event described here, with the reservations noted, may thus represent the first evidence for the returning closed flux produced in lobe reconnection at Saturn.

Cassini executed several rapid high latitude passes similar to that presented here during this mission phase. We have examined the three most similar passes surrounding the one on 25 June. While some show evidence

of a rather abrupt transition between the outer plasma sheet and the inner magnetosphere, none of them shows the clear evidence of injection-like plasma at that boundary. A more comprehensive survey is beyond the scope of the present work, so we are not able to make any generalizations about the frequency of occurrence of such plasmapause formation events.

4. Summary

The rapid high-latitude pass from lobe to inner magnetosphere on 25 June 2009 provides strong evidence for the formation of a plasmapause at Saturn by Vasyliunas-type reconnection of previously mass-loaded flux tubes. The region of hot, tenuous plasma that lies between the lobe and the dense inner magnetospheric plasma is consistent with a "cushion" region formed by very recent injection from a reconnection region in the tail, including low density, high temperature, supercorotational flow, a significant O^+ content, and the near-simultaneous observation of enhanced SKR emissions. The sharp boundary between that region and the cool dense inner magnetospheric plasma thus separates flux tubes that were involved in the reconnection from those that successfully traversed the nightside without mass loss. This event demonstrates that tail reconnection can strip off inner magnetospheric plasma in to at least a dipole L of 8.6. This newly created plasmapause is very likely unstable to centrifugally driven interchange, and we find clear evidence of exchanged flux tubes, both the inward moving hotter population and, for the first time, the outward moving cool population. The outward moving cool regions have azimuthal sizes less than 1 R_S, were probably created within the past 1.2 h, and have outflow speeds greater than about 5 km/s. We also find the possible signature of Dungey-type lobe reconnection pursuant to the initial Vasyliunas-type reconnection. Observations from the 25 June event are entirely consistent with previously described global MHD simulations of tail reconnection, plasmoid departure, and Saturnward injection of reconnected flux.

Acknowledgments

This work was stimulated by discussions held during two meetings of the International Space Science Institute (ISSI) team on "Modes of Radial Transport in Magnetospheres." Work at PSI was supported by the NASA Cassini program through JPL contract 1243218 with Southwest Research Institute. The Cassini project is managed by the Jet Propulsion Laboratory for NASA. M.F.T. is grateful to Los Alamos National Laboratory for the support provided her as a guest scientist. X.J. acknowledges support by the NASA Cassini mission through JPL contract 1409449 with the University of Michigan. C.M.J.'s work at Southampton was supported by a Science and Technology Facilities Council Ernest Rutherford Fellowship. Work at UCL-MSSL was supported by STFC, UK. The CAPS and MIMI distributions, the magnetic field values, and the RPWS power spectra shown in this analysis are available from the Planetary Data System (http://pds.nasa.gov/). The plasma moments are available as a prepeer-reviewed PDS data set.

Larry Kepko thanks Jerry Goldstein and another reviewer for their assistance in evaluating this paper.

References

André, N., et al. (2007), Magnetic signatures of plasma-depleted flux tubes in the Saturnian inner magnetosphere, *Geophys. Res. Lett.*, *34*, L14108, doi:10.1029/2007GL030374.

Brice, N. M., and G. A. Ioannidis (1970), The magnetospheres of Jupiter and Earth, *Icarus*, *13*, 173–183.

Bunce, E. J., S. W. H. Cowley, and J. A. Wild (2003), Azimuthal magnetic fields in Saturn's magnetosphere: Effects associated with plasma sub-corotation and magnetopause-tail current system, *Ann. Geophys.*, *21*, 1709.

Bunce, E. J., et al. (2005), In situ observations of a solar wind compression-induced hot plasma injection in Saturn's tail, *Geophys. Res. Lett.*, *32*, L20S04, doi:10.1029/2005GL022888.

Chen, Y., and T. W. Hill (2008), Statistical analysis of injection/dispersion events in Saturn's inner magnetosphere, *J. Geophys. Res.*, *113*, A07215, doi:10.1029/2008JA013166.

Dougherty, M. K., et al. (2004), The Cassini magnetic field investigation, *Space Sci. Rev.*, *114*, 331–383.

Gurnett, D. A., et al. (2004), The Cassini radio and plasma wave investigation, *Space Sci. Rev.*, *114*, 395–463.

Gurnett, D. A., et al. (2010), A plasmapause-like density boundary at high latitudes in Saturn's magnetosphere, *Geophys. Res. Lett.*, *37*, L16806, doi:10.1029/2010GL044466.

Jackman, C. M., and C. S. Arridge (2011), Statistical properties of the magnetic field in the Kronian magnetotail lobes and current sheet, *J. Geophys. Res.*, *116*, A05224, doi:10.1029/2010JA015973.

Jackman, C. M., et al. (2009), On the character and distribution of lower-frequency radio emissions at Saturn, and their relationship to substorm-like events, *J. Geophys. Res.*, *114*, A08211, doi:10.1029/2008JA013997.

Jackman, C. M., J. A. Slavin, and S. W. H. Cowley (2011), Cassini observations of plasmoid structure and dynamics: Implications for the role of magnetic reconnection in magnetospheric circulation at Saturn, *J. Geophys. Res.*, *116*, A10212, doi:10.1029/2011JA016682.

Jackman, C. M., N. Achilleos, S. W. H. Cowley, E. J. Bunce, A. Radioti, D. Grodent, S. V. Badman, M. K. Dougherty, and W. Pryor (2013), Auroral counterpart of magnetic field dipolarizations in Saturn's tail, *Planet. Space Sci.*, *82–83*, 34–42, doi:10.1016/j.pss.2013.03.010.

Jackman, C. M., et al. (2014), Saturn's dynamic magnetotail: A comprehensive magnetic field and plasma survey of plasmoids and traveling compression regions and their role in global magnetospheric dynamics, *J. Geophys. Res. Space Physics*, *119*, 5465–5494, doi:10.1002/2013JA019388.

Jia, X., et al. (2012), Magnetospheric configuration and dynamics of Saturn's magnetosphere: A global MHD simulation, *J. Geophys. Res.*, *117*, A05225, doi:10.1029/2012JA017575.

Kane, M., et al. (2014), Plasma convection in the nightside magnetosphere of Saturn determined from energetic ion anisotropies, *Planet. Space Sci.*, *91*, 1–13.

Khurana, K. K., and M. G. Kivelson (1993), Inference of the angular velocity of plasma in the Jovian magnetosphere from the sweepback of magnetic field, *J. Geophys. Res.*, *98*(A1), 67–79, doi:10.1029/92JA01890.

Kivelson, M. G., and D. J. Southwood (2005), Dynamical consequences of two modes of centrifugal instability in Jupiter's outer magnetosphere, *J. Geophys. Res.*, *110*, A12209, doi:10.1029/2005JA011176.

Krimigis, S. M., et al. (2004), Magnetosphere imaging instrument (MIMI) on the Cassini mission to Saturn/Titan, *Space Sci. Rev.*, *114*, 233–329.

Lamy, L., et al. (2008), Saturn kilometric radiation: Average and statistical properties, *J. Geophys. Res.*, *113*, A07201, doi:10.1029/2007JA012900.

Lewis, G. R., et al. (2008), Derivation of density and temperature from the Cassini-Huygens CAPS Electron Spectrometer, *Planet. Space Sci.*, *56*(7), 901–912, doi:10.1016/j.pss.2007.12.017.

Liu, X., et al. (2010), Numerical simulation of plasma transport in Saturn's inner magnetosphere using the Rice Convection Model, *J. Geophys. Res.*, *115*, A12254, doi:10.1029/2010JA015859.
Masters, A., et al. (2011), Supercorotating return flow from reconnection in Saturn's magnetotail, *Geophys. Res. Lett.*, *38*, L03103, doi:10.1029/2010GL046149.
McAndrews, H. J., et al. (2009), Plasma in Saturn's nightside magnetosphere and implications for global circulation, *Planet. Space Sci.*, *57*, 1714–1722; correction (2014), *Planet Space Sci.*, *97*, 86–87, doi:10.1016/j.pss/2014.05.011.
Mitchell, D. G., et al. (2005), Energetic ion acceleration in Saturn's magnetotail: Substorms at Saturn?, *Geophys. Res. Lett.*, *32*, L20S01, doi:10.1029/2005GL022647.
Mitchell, D. G., et al. (2009), Recurrent energization of plasma in the midnight-to-dawn quadrant of Saturn's magnetosphere, and its relationship to auroral UV and radio emissions, *Planet. Space Sci.*, *57*, 1732–1742.
Mitchell, D. G., et al. (2015), Injection, interchange, and reconnection: Energetic particle observations in Saturn's magnetosphere, in *Magnetotails in the Solar System*, *Geophys. Monogr. Ser.*, vol. 207, edited by A. Keiling, C. M. Jackman, and P. A. Delamere, pp. 327–344, John Wiley, Hoboken, N. J., doi:10.1002/9781118842324.ch19.
Nishida, A. (1966), Formation of plasmapause, or magnetospheric plasma knee, by the combined action of magnetospheric convection and plasma escape from the tail, *J. Geophys. Res.*, *71*, 5669–5679, doi:10.1029/JZ071i023p05669.
Russell, C. T., et al. (2008), Titan's influence on Saturnian substorm occurrence, *Geophys. Res. Lett.*, *35*, L15101, doi:10.1029/2008GL034080.
Sandel, B. R., et al. (2001), Initial results from the IMAGE Extreme Ultraviolet Imager, *Geophys. Res. Lett.*, *28*, 1439–1442, doi:10.1029/2001GL012885.
Schippers, P., et al. (2008), Multi-instrument analysis of electron populations in Saturn's magnetosphere, *J. Geophys. Res.*, *113*, A07208, doi:10.1029/2008JA013098.
Thomsen, M. F. (2013), Saturn's magnetospheric dynamics, *Geophys. Res. Lett.*, *40*, 5337–5344, doi:10.1002/2013GL057967.
Thomsen, M. F., et al. (2010), Survey of ion plasma parameters in Saturn's magnetosphere, *J. Geophys. Res.*, *115*, A10220, doi:10.1029/2010JA015267.
Thomsen, M. F., et al. (2013), Cassini/CAPS observations of duskside tail dynamics at Saturn, *J. Geophys. Res. Space Physics*, *118*, 5767–5781, doi:10.1002/jgra.50552.
Thomsen, M. F., et al. (2014a), Plasma flows in Saturn's nightside magnetosphere, *J. Geophys. Res. Space Physics*, *119*, 4521–4535, doi:10.1002/2014JA019912.
Thomsen, M. F., et al. (2014b), Ion composition in interchange injection events in Saturn's magnetosphere, *J. Geophys. Res. Space Physics*, *119*, 9761–9772, doi:10.1002/2014JA020489.
Vasyliunas, V. M. (1983), Plasma distribution and flow, in *Physics of the Jovian Magnetosphere*, edited by A. J. Dessler, pp. 395–453, Cambridge Univ. Press, New York.
Went, D. R., et al. (2011), Outer magnetospheric structure: Jupiter and Saturn compared, *J. Geophys. Res.*, *116*, A04224, doi:10.1029/2010JA016045.
Wilson, R. J., et al. (2008), Cassini plasma spectrometer thermal ion measurements in Saturn's inner magnetosphere, *J. Geophys. Res.*, *113*, A12218, doi:10.1029/2008JA013486.
Wilson, R. J., R. L. Tokar, and M. G. Henderson (2009), Thermal ion flow in Saturn's inner magnetosphere measured by the Cassini plasma spectrometer: A signature of the Enceladus torus?, *Geophys. Res. Lett.*, *36*, L23104, doi:10.1029/2009GL040225.
Young, D. T., et al. (2004), Cassini plasma spectrometer investigation, *Space Sci. Rev.*, *114*, 1–112.
Young, D. T., et al. (2005), Composition and dynamics of plasma in Saturn's magnetosphere, *Science*, *307*, 1262–1266.
Zieger, B., et al. (2010), Periodic plasma escape from the mass-loaded Kronian magnetosphere, *J. Geophys. Res.*, *115*, A08208, doi:10.1029/2009JA014951.